

# A multi-class mean-excess traffic equilibrium model with elastic demand

Xiangdong Xu<sup>1,2\*</sup>, Anthony Chen<sup>2</sup>, Zhong Zhou<sup>3</sup> and Lin Cheng<sup>1</sup>

<sup>1</sup>School of Transportation, Southeast University, Nanjing 210096, China

<sup>2</sup>Department of Civil and Environmental Engineering, Utah State University, Logan, UT 84322-4110, USA

<sup>3</sup>Citilabs, 316 Williams Street, Tallahassee, FL 32303, USA

## SUMMARY

Recent empirical studies have revealed that travel time variability plays an important role in travelers' route choice decisions. To simultaneously account for both reliability and unreliability aspects of travel time variability, the concept of mean-excess travel time (METT) was recently proposed as a new risk-averse route choice criterion. In this paper, we extend the mean-excess traffic equilibrium model to include heterogeneous risk-aversion attitudes and elastic demand. Specifically, this model explicitly considers (1) multiple user classes with different risk-aversions toward travel time variability when making *route choice* decisions under uncertainty and (2) the elasticity of travel demand as a function of METT when making *travel choice* decisions under uncertainty. This model is thus capable of modeling travelers' heterogeneous risk-averse behaviors with both travel choice and route choice considerations. The proposed model is formulated as a variational inequality problem and solved via a route-based algorithm using the modified alternating direction method. Numerical analyses are also provided to illustrate the features of the proposed model and the applicability of the solution algorithm. Copyright © 2012 John Wiley & Sons, Ltd.

KEY WORDS: mean-excess travel time; travel time budget; user equilibrium; multiple user classes; elastic demand; uncertainty

## 1. INTRODUCTION

Transportation systems have many uncertainties (e.g., demand fluctuation, capacity degradation), which aggregately result in travel time variability [1]. Recently, several empirical studies have revealed that travel time variability plays an important role in travelers' route choice decisions (e.g., [2,3]). Travelers treat travel time variability as a risk in their travel choices because it introduces uncertainty for an on-time arrival at the destination. Because of its theoretical and practical importance, modeling route choice behavior under uncertainty is becoming an emerging research subject. Some of the recent principal advances on this topic are listed in Table I, which highlights the aspects of travel time variability in consideration (e.g., reliability, unreliability, or both), the type of travel demand (e.g., fixed or elastic), the number of user classes (e.g., single or multiple), the source of uncertainty (e.g., demand, supply, or both), and the assumed probability distribution of uncertainty. Furthermore, this table also provides the route choice decision criterion (e.g., user equilibrium (UE) or stochastic user equilibrium), and the mathematical approach used in the formulation (e.g., mathematical programming, nonlinear complementarity problem, variational inequality (VI), or fixed point problem). For other route choice models under uncertainty, interested readers may refer to the game theory approach (e.g., [4]),

\*Correspondence to: Xiangdong Xu, School of Transportation, Southeast University, Nanjing 210096, China. E-mail: huoshanzhx@163.com

Table I. Some recent major route choice models under uncertainty.

Model	Reference	Decision criterion	Travel time variability	Model structure	Source of uncertainty	Dist. of uncertainty	Type of demand	User classes
TTB based	Lo <i>et al.</i> [8]	UE	Reliability	MP	Link capacity	Uniform	Fixed	Multiple
	Shao <i>et al.</i> [9]	UE	Reliability	VI	Demand	Normal	Elastic	Single
	Shao <i>et al.</i> [10]	SUE	Reliability	VI	Demand	Normal	Elastic	Multiple
	Siu and Lo [24]	UE and SUE	Reliability	NCP	Link capacity	Uniform	Fixed	Multiple
	Lam <i>et al.</i> [25]	SUE	Reliability	FP	Demand	Normal	Elastic	Single
Schedule delay based	Shao <i>et al.</i> [26]	SUE	Reliability	VI	Supply (adverse weather)	Generalized BPR	Elastic	Multiple
	Siu and Lo [27]	Mixed equilibrium	Reliability	NCP	Supply (adverse weather)	Generalized BPR	Fixed	Commuters and non-commuters
METT based	Watling [15]	UE	Unreliability	VI and NCP	Capacity	Uniform	Fixed	Single
	Chen and Zhou [16]	UE	Reliability and unreliability	VI	Any Demand	Multivariate normal Lognormal	Fixed	Single
	Chen <i>et al.</i> [28]	SUE	Reliability and unreliability	VI	Demand	Lognormal	Fixed	Single

TTB, travel time budget; BPR, Bureau of Public Roads; UE, user equilibrium; MP, mathematical programming; NCP, nonlinear complementarity problem; SUE, stochastic user equilibrium; VI, variational inequality; FP, fixed point; METT, mean-excess travel time.

utility-based approach (e.g., [5]), expected residual minimization approach [6], and prospect theory-based approach (e.g., [7]).

The models shown in Table I can be classified as the travel time budget (TTB)-based, schedule delay-based, and mean-excess travel time (METT)-based models according to the aspect(s) of travel time variability considered in the model:

- (1) TTB is defined as a travel time reliability chance constraint such that the probability that a trip can be completed within the threshold is not less than a user-specified confidence level  $\alpha$  [8–10]. It is composed of the mean travel time and a buffer time, similar to the concept of effective travel time used to ensure the user-specified travel time reliability requirement. However, it does not account for the unreliability aspect of travel time variability when the travelers are late (i.e., encountering worse travel times beyond the TTB in the distribution tail of  $1 - \alpha$ ). Recently, the TTB model is also adopted in transit assignment under uncertainty (e.g., [11–13]) and dynamic traffic assignment under uncertainty (e.g., [14]).
- (2) In order to consider the unreliability aspect of travel time variability, Watling [15] proposed a late arrival penalized user equilibrium model by incorporating a schedule delay term in a disutility function to penalize the late arrival for a *fixed* departure time (or a *fixed* TTB).
- (3) METT is defined to address two fundamental questions: “how long do I need to allow for this trip” and “how bad should I expect for the worse cases” [16]. It is considered as a more complete and accurate risk-averse measure to describe travelers’ route choice decisions under uncertainty because it simultaneously accounts for both reliability (on-time arrival) and unreliability (late arrival) aspects of travel time variability.

In the mean-excess traffic equilibrium (METE) model recently proposed by Chen and Zhou [16], they assume that the origin–destination (O-D) demand is fixed and given, and all travelers have the same risk attitude toward travel time variability in their route choice decisions. These assumptions are relaxed in this paper to better reflect the decision processes of multi-dimensional travel choices (i.e., whether to travel and which route to take). In this study, travel demand is affected by the risk-averse impedance of making a trip (i.e., the minimal METT between an O-D pair). A classic example is that when the O-D minimal METT during the peak period is greatly increased, part of the potential travelers may start their trips ahead of the usual departure time, postpone their departure time, or even cancel the trip plan. All these responses may result in decreasing the volumes of demand during the peak period.

Besides the dependence of travel demand on travel time variability, different travelers may respond to such variation of travel time differently depending on their risk preferences. Typically, travelers can be categorized as risk-prone, risk-neutral, and risk-averse according to their attitudes toward risk [5]. The risk in this context is travel time variability, which directly affects their decisions to travel during the peak period (i.e., demand for travel) and their decisions in selecting a route (e.g., a route with a low mean travel time and a high travel time variance versus another route with a high mean travel time and a low travel time variance). In addition, a risk-averse traveler will allocate a larger amount of travel time to more frequently ensure on-time arrivals and also to avoid late arrivals at his or her destination. Thus, it is necessary to explicitly account for the heterogeneous risk-averse travel behaviors and the impact of travel time variability (via METT) on the elastic demand in the METE modeling framework.

The objective of this paper is to develop a multi-class METE with elastic demand (MC-METE-ED) to consider both reliability (on-time arrival) and unreliability (late arrival) aspects of travel time variability when making travel choice decisions under uncertainty. This model is formulated as a VI problem and solved via a route-based algorithm using the modified alternating direction (MAD) method to obtain the equilibrium flow and demand patterns. The remainder of this paper is organized as follows. In Section 2, we provide the equilibrium conditions and the equivalent VI problem. A route-based MAD method is developed in Section 3. Section 4 presents some numerical examples to illustrate the essential ideas of the proposed model and the applicability of the solution algorithm. Finally, some concluding remarks are given in Section 5.

## 2. MATHEMATICAL MODEL

In this section, we present the descriptive conditions of MC-METE-ED, the equivalent VI formulation, and a special case of METT under the lognormal demand distribution.

2.1. Equilibrium conditions

Consider a transportation network  $G = [N, A]$ , where  $N$  and  $A$  denote the sets of nodes and links, respectively. Let  $W$  denote the set of O-D pairs for which travel demand  $q^w$  is generated between O-D pair  $w \in W$ , and let  $f_p^w$  denote the flow on route  $p \in P^w$ , where  $P^w$  is the set of routes connecting O-D pair  $w$  and all  $P^w$  constitute  $P$ . For completeness, we first present the definition of METT and then the MC-METE-ED conditions.

**Definition 1.** The METT  $\eta_p^w(\alpha)$  on route  $p$  between O-D pair  $w$  with respect to a predefined confidence level  $\alpha$  is defined as the conditional expectation of the random route travel time  $T_p^w$  exceeding the corresponding route TTB  $\xi_p^w(\alpha)$  [16], i.e.,

$$\eta_p^w(\alpha) = E \left[ T_p^w \mid T_p^w \geq \xi_p^w(\alpha) \right], \forall p \in P^w, w \in W, \tag{1}$$

where  $E[\cdot]$  is the expectation operator and  $\xi_p^w(\alpha)$  is defined by the following travel time reliability chance-constrained model:

$$\xi_p^w(\alpha) = \min \left\{ \xi \mid \Pr \left( T_p^w \leq \xi \right) \geq \alpha \right\} = E \left[ T_p^w \right] + \gamma_p^w(\alpha), \forall p \in P^w, w \in W, \tag{2}$$

where  $\gamma_p^w(\alpha)$  is a “buffer time” added to the mean travel time  $E \left[ T_p^w \right]$  to ensure the travel time reliability requirement for on-time arrivals at the confidence level  $\alpha$ .

Meanwhile, Equation (1) can be rewritten as:

$$\eta_p^w(\alpha) = \xi_p^w(\alpha) + E \left[ \left( T_p^w - \xi_p^w(\alpha) \right) \mid T_p^w \geq \xi_p^w(\alpha) \right], \forall p \in P^w, w \in W, \tag{3}$$

where the first and second terms represent the reliability (in terms of TTB) and unreliability (in terms of expected excess delay (EED)) aspects of route travel time variability, respectively. These two terms explicitly capture the left region of the travel time distribution with the  $\alpha$ -percentile reliability requirement and the right region with the  $(1 - \alpha)$  percentile of unreliability in the distribution tail, respectively. In this sense, METT considers both on-time arrival (via TTB) and late arrival (via EED) aspects, whereas TTB only considers on-time arrival requirement. It should be noted that for the convenience of explicitly presenting the composition of METT, we decompose METT into two terms (i.e., TTB and EED). However, these two terms are interdependent via the confidence level of  $\alpha$ .

In this study, we classify travelers according to their risk attitudes toward travel time variability using the confidence level  $\alpha$ . Different user classes have different confidence levels. However, we assume all travelers within a user class  $i \in I$  ( $I$  is the set of all user classes) have the same confidence level  $\alpha_i$ . Accordingly, the random travel demand  $Q^w$  is also divided into  $|I|$  user classes ( $|I|$  is the cardinality of  $I$ ). We denote the travel demand of a generic user class by  $Q_i^w, i \in I, w \in W$ . Descriptive conditions of the MC-METE-ED are defined as follows:

**Definition 2.** The MC-METE-ED is a network state such that for each user class, all used routes connecting an O-D pair have equal and minimal METT. Meanwhile, the actual travel demand between each O-D pair for each user class satisfies its corresponding elastic demand function.

For each user class, the METT on the used routes is not larger than that on any unused route connecting this O-D pair. In addition, the actual O-D demand for each user class depends on the minimal METT of this O-D pair and this user class. The earlier descriptive conditions can be mathematically stated as

$$\eta_{p,i}^w(\mathbf{f}^*) \begin{cases} = u_i^w, & \text{if } (f_{p,i}^w)^* > 0 \\ \geq u_i^w, & \text{if } (f_{p,i}^w)^* = 0 \end{cases}, \forall p \in P^w, w \in W, i \in I, \tag{4}$$

$$(q_i^w)^* = D_i^w(u_i^w), \forall w \in W, i \in I, \tag{5}$$

where  $\eta_{p,i}^w$  and  $f_{p,i}^w$  are the METT and flow of user class  $i$  on route  $p$  between O-D pair  $w$ , respectively;  $u_i^w, q_i^w$ , and  $D_i^w(\cdot)$  are the minimal METT, actual demand, and elastic demand function of user class  $i$  between O-D

pair  $w$ , respectively. We further assume that the travel demand function between each O-D pair  $w$  for each user class  $i$ ,  $D_i^w(\cdot)$ , is a monotonically decreasing function of its corresponding minimal METT,  $u_i^w$ . This assumption guarantees  $q_i^w = D_i^w(u_i^w)$  is invertible. Note that although the travel demand function is separable, non-separable elastic demand functions (including symmetric and asymmetric forms) can also be used in this model.

Accordingly, Equations (4) and (5) can also be rewritten as the following complementarity system of equations:

$$f_{p,i}^w (\eta_{p,i}^w - u_i^w) = 0, \forall p \in P^w, w \in W, i \in I, \tag{6}$$

$$\eta_{p,i}^w - u_i^w \geq 0, \forall p \in P^w, w \in W, i \in I, \tag{7}$$

$$f_{p,i}^w \geq 0, \forall p \in P^w, w \in W, i \in I, \tag{8}$$

$$q_i^w (u_i^w - D_i^{w,-1}(q_i^w)) = 0, \forall w \in W, i \in I, \tag{9}$$

$$u_i^w - D_i^{w,-1}(q_i^w) \geq 0, \forall w \in W, i \in I, \tag{10}$$

$$q_i^w \geq 0, \forall w \in W, i \in I, \tag{11}$$

$$\sum_{p \in P^w} f_{p,i}^w = q_i^w, \forall w \in W, i \in I, \tag{12}$$

where  $D_i^{w,-1}(q_i^w)$  is the inverse demand function of user class  $i$  between O-D pair  $w$ . Equations (6)–(8) are the METT-based UE conditions for each user class and each O-D pair. That is, for each user class, if a route is used, then the route METT is equal to the minimal METT between this O-D pair, while the unused route will not have a lower METT. Equations (9) and (10) imply that if the O-D demand for a user class is positive, then the corresponding minimal METT and the actual O-D demand satisfy the elastic demand function. On the contrary, if the minimal METT is greater than the O-D cost obtained from the inverse demand function, then no user is willing to travel. Equation (11) is the non-negativity constraint of the actual travel demand, and Equation (12) is the flow conservation constraint.

### 2.2. Variational inequality formulation

The aforementioned equilibrium conditions can be equivalently formulated as the following VI problem, which is to find a route flow and demand pattern  $(\mathbf{f}^*, \mathbf{q}^*) \in \Omega_{\mathbf{f}\mathbf{q}}$ , such that

$$\begin{aligned} & \sum_{i \in I} \sum_{w \in W} \sum_{p \in P^w} \eta_{p,i}^w(\mathbf{f}^*) \cdot (f_{p,i}^w - (f_{p,i}^w)^*) - \\ & \sum_{i \in I} \sum_{w \in W} D_i^{w,-1}(\mathbf{q}^*) \cdot (q_i^w - (q_i^w)^*) \geq 0, \forall (\mathbf{f}, \mathbf{q}) \in \Omega_{\mathbf{f}\mathbf{q}}, \end{aligned} \tag{13}$$

where  $\Omega_{\mathbf{f}\mathbf{q}}$  is the feasible set defined as follows:

$$\sum_{p \in P^w} f_{p,i}^w = q_i^w, \forall w \in W, i \in I, \tag{14}$$

$$f_{p,i}^w \geq 0, \forall p \in P^w, w \in W, i \in I, \tag{15}$$

$$q_i^w \geq 0, \forall w \in W, i \in I. \tag{16}$$

For conciseness, the aforementioned VI problem given in Equations(13)–(16) can also be written in the following compact vector form:

$$\boldsymbol{\eta}(\mathbf{f}^*)^T(\mathbf{f} - \mathbf{f}^*) - \mathbf{D}^{-1}(\mathbf{q}^*)^T(\mathbf{q} - \mathbf{q}^*) \geq 0, \forall (\mathbf{f}, \mathbf{q}) \in \Omega_{\mathbf{f}\mathbf{q}}, \quad (17)$$

where the feasible set  $\Omega_{\mathbf{f}\mathbf{q}}$  in vector form is,

$$\Omega_{\mathbf{f}\mathbf{q}} = \{(\mathbf{f}, \mathbf{q}) | \boldsymbol{\Lambda}\mathbf{f} = \mathbf{q}, \mathbf{f} \geq \mathbf{0}, \mathbf{q} \geq \mathbf{0}\}, \quad (18)$$

where  $\boldsymbol{\Lambda}$  is the O-D pair-route incidence matrix. The dimensions of the vectors  $\mathbf{f} = (\dots, f_{p,i}^w, \dots)^T$ ,  $\mathbf{q} = (\dots, q_i^w, \dots)^T$ ,  $\boldsymbol{\eta} = (\dots, \eta_{p,i}^w, \dots)^T$ , and  $\mathbf{u} = (\dots, u_i^w, \dots)^T$  are  $|I| \cdot |P|$ ,  $|I| \cdot |W|$ ,  $|I| \cdot |P|$ , and  $|I| \cdot |W|$ , respectively.

For the existence of a solution to this VI problem and its equivalence to the MC-METE-ED, please refer to Appendix A. It is necessary to point out that the uniqueness of the equilibrium route flow solution cannot be guaranteed. In order to prove the uniqueness, strict monotonicity of the mapping is required. However, it is difficult to guarantee the monotonicity of the non-additive route METT with respect to route flows in general.

### 2.3. Mean-excess travel time under the lognormal travel demand distribution

In this section, we provide a special case of the analytical METT expression under the lognormal distributed demand uncertainty. Note that the lognormal distribution has been extensively used in general reliability applications to model failure times. It can capture the asymmetric and skewed characteristics of a probability distribution. For the lognormal distributed travel demand, the probability distribution of the random route travel time can be derived as shown in Table II, where we use the following Bureau of Public Roads (BPR)-type link performance function:

$$t_a = t_a^0 [1 + \beta(v_a/C_a)^n], \forall a \in A, \quad (19)$$

where  $t_a$ ,  $t_a^0$ ,  $v_a$ , and  $C_a$  are the travel time, free-flow travel time, flow, and capacity on link  $a$ , respectively.  $\beta$  and  $n$  are BPR parameters. From the route travel time distribution shown in Table II, the expressions for calculating TTB  $\zeta_{p,i}^w(\alpha_i)$  and METT  $\eta_{p,i}^w(\alpha_i)$  at a certain confidence level  $\alpha_i$  can be derived as follows:

$$\zeta_{p,i}^w(\alpha_i) = t_p^w + \Phi^{-1}(\alpha_i) \cdot \sigma_{p,t}^w, \forall p \in P^w, w \in W, i \in I, \quad (20)$$

$$\begin{aligned} \eta_{p,i}^w(\alpha_i) &= \zeta_{p,i}^w(\alpha_i) + \left( \frac{\sigma_{p,t}^w}{\sqrt{2\pi}(1-\alpha_i)} \cdot \exp\left(-\frac{(\Phi^{-1}(\alpha_i))^2}{2}\right) - \Phi^{-1}(\alpha_i) \cdot \sigma_{p,t}^w \right) \\ &= t_p^w + \frac{\sigma_{p,t}^w}{\sqrt{2\pi}(1-\alpha_i)} \cdot \exp\left(-\frac{(\Phi^{-1}(\alpha_i))^2}{2}\right), \forall p \in P^w, w \in W, i \in I, \end{aligned} \quad (21)$$

where  $t_p^w$  and  $\sigma_{p,t}^w$  are the mean and standard deviation of the travel time on route  $p$  between O-D pair  $w$ , respectively, and  $\Phi^{-1}(\cdot)$  is the inverse of the standard normal cumulative distribution function. For details of the derivation, interested readers may refer to Chen and Zhou [16] and Zhou and Chen [17]. For the normally distributed travel demand, please refer to Shao *et al.* [10] for the derivation of the analytical TTB expression.

## 3. ROUTE-BASED SOLUTION ALGORITHM

The METT in the proposed VI problem is non-additive because it is not possible to decompose the route METT into the sum of link-based generalized costs. Thus, the commonly used link-based traffic assignment algorithms, such as the well-known Frank-Wolfe algorithm are not applicable. Considering the special structure of this VI problem, we adopt a route-based algorithm using the MAD method to obtain the equilibrium route flow and O-D demand pattern. The MAD method is attractive for solving large-scale structured VI problems where the feasible set is an intersection between a simple set and a polyhedron (see Han [18] for the convergence property). In this paper, we extend the MAD method

Table II. Distributions of flow and travel time.

Measure	Distribution	Parameters	Mean	Variance
Travel demand	$Q^w \sim \text{LN}(\mu_q^w, \sigma_q^w)$	$\mu_q^w = \ln(q^w) - \frac{1}{2} \ln(1 + \varepsilon^w / (q^w)^2)$ $(\sigma_q^w)^2 = \ln(1 + \varepsilon^w / (q^w)^2)$	$q^w$	$\varepsilon^w$
Route flow	$F_p^w \sim \text{LN}(\mu_{p,f}^w, \sigma_{p,f}^w)$	$\mu_{p,f}^w = \ln(f_p^w) - \frac{1}{2} \ln(1 + \varepsilon_{p,f}^w / (f_p^w)^2)$ $(\sigma_{p,f}^w)^2 = \ln(1 + \varepsilon_{p,f}^w / (f_p^w)^2)$	$f_p^w = \sum_i f_{p,i}^w$	$\varepsilon_{p,f}^w = f_p^w \cdot \frac{\varepsilon^w}{q^w}$
Link flow	$V_a \sim \text{LN}(\mu_{a,v}^w, \sigma_{a,v}^w)$	$\mu_{a,v}^w = \ln(v_a) - \frac{1}{2} \ln(1 + \varepsilon_{a,v}^w / (v_a)^2)$ $(\sigma_{a,v}^w)^2 = \ln(1 + \varepsilon_{a,v}^w / (v_a)^2)$	$v_a = \sum_w \sum_{p \neq a} f_{pa}^{w,S}$	$\varepsilon_{a,v}^w = \sum_w \sum_{p \neq a} f_{pa}^{w,S} \frac{\varepsilon^w}{q^w}$
Link travel time	N/A	N/A	$t_a = t_a^0 + \frac{\beta t_a^0}{(C_a)^n}$ $\exp\left(n\mu_{a,v}^w + \frac{n^2(\sigma_{a,v}^w)^2}{2}\right)$	$\varepsilon_{a,t}^w = \left(\frac{\beta t_a^0}{(C_a)^n}\right)^2 \cdot \exp\left(n^2(\sigma_{a,v}^w)^2\right) - 1$ $\exp\left(2n\mu_{a,v}^w + n^2(\sigma_{a,v}^w)^2\right)$
Route travel time	$T_p^w \sim N\left(t_p^w, (\sigma_{p,t}^w)^2\right)$ (Central Limit Theorem)	$t_p^w = \sum_a t_{a,p}^w$ $\sigma_{p,t}^w = \sqrt{\varepsilon_{p,t}^w}$	$t_p^w = \sum_a t_{a,p}^w$	$\varepsilon_{p,t}^w = \sum_a \varepsilon_{a,t}^w \frac{\delta_{pa}^w}{p_a}$

LN, lognormal distribution; N, normal distribution; N/A, not applicable.

developed by Chen and Zhou [16] to solve the MC-METE-ED model. We should point out that the solution vectors in this paper include both the route flows and travel demands for each user class. These considerations make the VI problem more complicated to solve compared with that in Chen and Zhou [16], especially on the descent direction, step-size determination, and convergence criterion.

After attaching a Lagrangian multiplier vector  $\boldsymbol{\pi}$  for the conservation constraint in Equation (14), the original VI problem can be rewritten as follows:

$$\mathbf{F}(\mathbf{x}^*)^T(\mathbf{x} - \mathbf{x}^*) \geq 0, \forall \mathbf{x} \in \Omega_{\mathbf{x}}, \tag{22}$$

where

$$\mathbf{x} = \begin{pmatrix} \mathbf{f} \\ \mathbf{q} \\ \boldsymbol{\pi} \end{pmatrix} \in \Omega_{\mathbf{x}} = \left( R_+^{|\mathcal{P}| \cdot |\mathcal{I}|} \times R_+^{|\mathcal{W}| \cdot |\mathcal{I}|} \times R^{|\mathcal{W}| \cdot |\mathcal{I}|} \right), \quad \mathbf{F}(\mathbf{x}) = \begin{pmatrix} \boldsymbol{\eta}(\mathbf{f}) - \boldsymbol{\Lambda}^T \boldsymbol{\pi} \\ -\mathbf{D}^{-1}(\mathbf{q}) + \boldsymbol{\pi} \\ \boldsymbol{\Lambda} \mathbf{f} - \mathbf{q} \end{pmatrix}. \tag{23}$$

At this time,  $\mathbf{f} \in R_+^{|\mathcal{P}| \cdot |\mathcal{I}|}$  because the conservation constraint has been eliminated. The new feasible set  $\Omega_{\mathbf{x}}$  in Equation (22) is just an intersection of two non-negative orthants and a Euclidean space. This manipulation facilitates the projection operations on the new simple feasible set. The solution procedure of the MAD method is presented as follows.

**Step 0: Initialization and parameter setting.**

- (1) Set values for parameters: tolerance error  $\varepsilon$ , initial inner loop step-size  $\beta_0$ , its scaling factor  $\mu \in (0,1)$ , adjusting factors  $\nu \in (0,1)$ ,  $\delta \in (0,1)$ , and scaling parameter  $\gamma \in (0,2)$  for updating the iterative solution.
- (2) Set an initial solution  $\mathbf{x}^0 \in \Omega_{\mathbf{x}}$  where the only requirement is  $\mathbf{f}^0 \geq \mathbf{0}$ ,  $\mathbf{q}^0 \geq \mathbf{0}$ .
- (3) Set the iteration counter  $k := 0$ .

**Step 1: Compute the METT  $\boldsymbol{\eta}(\mathbf{f}^k)$  and the inverse demand function  $-\mathbf{D}^{-1}(\mathbf{q}^k)$ .**

**Step 2: Check convergence.** Calculate the Euclidian norm  $\|\mathbf{r}(\mathbf{x}^k, \beta_k)\|$ , where

$$\begin{aligned} \mathbf{r}(\mathbf{x}^k, \beta_k) &= \mathbf{x}^k - P_{\Omega_{\mathbf{x}}}[\mathbf{x}^k - \beta_k \mathbf{F}(\mathbf{x}^k, \beta_k)], \text{ i.e.,} \\ \begin{pmatrix} \mathbf{r}_1(\mathbf{x}^k, \beta_k) \\ \mathbf{r}_2(\mathbf{x}^k, \beta_k) \\ \mathbf{r}_3(\mathbf{x}^k, \beta_k) \end{pmatrix} &= \begin{pmatrix} \mathbf{f}^k - P_{R_+^{|\mathcal{P}| \cdot |\mathcal{I}|}}[\mathbf{f}^k - \beta_k(\boldsymbol{\eta}(\mathbf{f}^k) - \boldsymbol{\Lambda}^T(\boldsymbol{\pi}^k - \beta_k(\boldsymbol{\Lambda} \mathbf{f}^k - \mathbf{q}^k)))] \\ \mathbf{q}^k - P_{R_+^{|\mathcal{W}| \cdot |\mathcal{I}|}}[\mathbf{q}^k - \beta_k(-\mathbf{D}^{-1}(\mathbf{q}^k) + (\boldsymbol{\pi}^k - \beta_k(\boldsymbol{\Lambda} \mathbf{f}^k - \mathbf{q}^k)))] \\ \beta_k(\boldsymbol{\Lambda} \mathbf{f}^k - \mathbf{q}^k) \end{pmatrix}. \end{aligned}$$

If  $\max\{\|\mathbf{r}(\mathbf{x}^k, \beta_k)\|/\beta_k, \|\mathbf{r}(\mathbf{x}^k, \beta_k)\|\} < \varepsilon$ , then stop and set  $\mathbf{x}^* := \mathbf{x}^k$ ; otherwise, find the smallest non-negative integer  $m_k$  such that  $\beta_k = \beta_k \cdot \mu^{m_k}$  satisfying

$$\begin{aligned} &\beta_k(\mathbf{r}_1(\mathbf{x}^k, \beta_k))^T[\boldsymbol{\eta}(\mathbf{f}^k) - \boldsymbol{\eta}(\bar{\mathbf{f}}^k)] + \beta_k(\mathbf{r}_2(\mathbf{x}^k, \beta_k))^T[-\mathbf{D}^{-1}(\mathbf{q}^k) + \mathbf{D}^{-1}(\bar{\mathbf{q}}^k)] + \\ &\beta_k(\mathbf{r}_3(\mathbf{x}^k, \beta_k))^T \boldsymbol{\Lambda} \mathbf{r}_1(\mathbf{x}^k, \beta_k) - \beta_k(\mathbf{r}_3(\mathbf{x}^k, \beta_k))^T \mathbf{r}_2(\mathbf{x}^k, \beta_k) \leq \\ &\delta(\|\mathbf{r}_1(\mathbf{x}^k, \beta_k)\|^2 + \|\mathbf{r}_2(\mathbf{x}^k, \beta_k)\|^2), \end{aligned}$$

where  $\bar{\mathbf{f}}^k = P_{R_+^{|\mathcal{P}| \cdot |\mathcal{I}|}}[\mathbf{f}^k - \beta_k(\boldsymbol{\eta}(\mathbf{f}^k) - \boldsymbol{\Lambda}^T(\boldsymbol{\pi}^k - \beta_k(\boldsymbol{\Lambda} \mathbf{f}^k - \mathbf{q}^k)))]$ , and  $\bar{\mathbf{q}}^k = P_{R_+^{|\mathcal{W}| \cdot |\mathcal{I}|}}[\mathbf{q}^k - \beta_k(-\mathbf{D}^{-1}(\mathbf{q}^k) + (\boldsymbol{\pi}^k - \beta_k(\boldsymbol{\Lambda} \mathbf{f}^k - \mathbf{q}^k)))]$ .

**Step 3: Compute  $\bar{\boldsymbol{\pi}}^k = \boldsymbol{\pi}^k - \beta_k(\boldsymbol{\Lambda} \bar{\mathbf{f}}^k - \bar{\mathbf{q}}^k)$ .**

**Step 4: Find the descent direction  $-\mathbf{d}(\mathbf{x}^k, \beta_k)$ .**

$$\mathbf{d}(\mathbf{x}^k, \beta_k) = \begin{pmatrix} \mathbf{r}_1(\mathbf{x}^k, \beta_k) - \beta_k[\boldsymbol{\eta}(\mathbf{f}^k) - \boldsymbol{\eta}(\bar{\mathbf{f}}^k)] - \beta_k \boldsymbol{\Lambda}^T \mathbf{r}_3(\mathbf{x}^k, \beta_k) \\ \mathbf{r}_2(\mathbf{x}^k, \beta_k) - \beta_k[-\mathbf{D}^{-1}(\mathbf{q}^k) + \mathbf{D}^{-1}(\bar{\mathbf{q}}^k)] + \beta_k \mathbf{r}_3(\mathbf{x}^k, \beta_k) \\ \mathbf{r}_3(\mathbf{x}^k, \beta_k) - \beta_k \boldsymbol{\Lambda} \mathbf{r}_1(\mathbf{x}^k, \beta_k) + \beta_k \mathbf{r}_2(\mathbf{x}^k, \beta_k) \end{pmatrix}.$$

(Continues)

**Step 5: Find the step-size in the outer loop**  $\rho(\mathbf{x}^k, \beta_k)$ .

$$\begin{aligned} \rho(\mathbf{x}^k, \beta_k) &= \frac{\varphi(\mathbf{x}^k, \beta_k)}{\|\mathbf{d}(\mathbf{x}^k, \beta_k)\|^2}, \text{ where } \varphi(\mathbf{x}^k, \beta_k) = \|\mathbf{r}_1(\mathbf{x}^k, \beta_k)\|^2 + \|\mathbf{r}_2(\mathbf{x}^k, \beta_k)\|^2 \\ &\quad - \beta_k(\mathbf{r}_1(\mathbf{x}^k, \beta_k))^T [\boldsymbol{\eta}(\mathbf{f}^k) - \boldsymbol{\eta}(\bar{\mathbf{f}}^k)] - \beta_k(\mathbf{r}_2(\mathbf{x}^k, \beta_k))^T [-\mathbf{D}^{-1}(\mathbf{q}^k) + \mathbf{D}^{-1}(\bar{\mathbf{q}}^k)] \\ &\quad - \beta_k(\mathbf{r}_3(\mathbf{x}^k, \beta_k))^T \boldsymbol{\Lambda} \mathbf{r}_1(\mathbf{x}^k, \beta_k) + \beta_k(\mathbf{r}_3(\mathbf{x}^k, \beta_k))^T \mathbf{r}_2(\mathbf{x}^k, \beta_k) \end{aligned}$$

**Step 6: Update the iterative solution**  $\mathbf{x}^{k+1} = P_{\Omega_x}[\mathbf{x}^k - \gamma\rho(\mathbf{x}^k, \beta_k)\mathbf{d}(\mathbf{x}^k, \beta_k)]$ , i.e.,

$$\begin{pmatrix} \mathbf{f}^{k+1} \\ \mathbf{q}^{k+1} \\ \boldsymbol{\pi}^{k+1} \end{pmatrix} = \begin{pmatrix} \max\{\mathbf{0}, \mathbf{f}^k - \gamma\rho(\mathbf{x}^k, \beta_k)\mathbf{d}_1(\mathbf{x}^k, \beta_k)\} \\ \max\{\mathbf{0}, \mathbf{q}^k - \gamma\rho(\mathbf{x}^k, \beta_k)\mathbf{d}_2(\mathbf{x}^k, \beta_k)\} \\ \boldsymbol{\pi}^k - \gamma\rho(\mathbf{x}^k, \beta_k)\mathbf{d}_3(\mathbf{x}^k, \beta_k) \end{pmatrix}.$$

**Step 7: Update the step-size in the inner loop**  $\beta_{k+1}$ . If

$$\begin{aligned} &\beta_k(\mathbf{r}_1(\mathbf{x}^k, \beta_k))^T [\boldsymbol{\eta}(\mathbf{f}^k) - \boldsymbol{\eta}(\bar{\mathbf{f}}^k)] + \beta_k(\mathbf{r}_2(\mathbf{x}^k, \beta_k))^T [-\mathbf{D}^{-1}(\mathbf{q}^k) + \mathbf{D}^{-1}(\bar{\mathbf{q}}^k)] + \\ &\beta_k(\mathbf{r}_3(\mathbf{x}^k, \beta_k))^T \boldsymbol{\Lambda} \mathbf{r}_1(\mathbf{x}^k, \beta_k) - \beta_k(\mathbf{r}_3(\mathbf{x}^k, \beta_k))^T \mathbf{r}_2(\mathbf{x}^k, \beta_k) \geq \\ &v(\|\mathbf{r}_1(\mathbf{x}^k, \beta_k)\|^2 + \|\mathbf{r}_2(\mathbf{x}^k, \beta_k)\|^2), \end{aligned}$$

then set  $\beta_{k+1} = \beta_k/\mu$ ; else, set  $\beta_{k+1} = \beta_k$ . Set  $k:=k+1$  and go to Step 1.

---

The MAD method mainly consists of an inner loop and an outer loop. The inner loop is to find a suitable auxiliary solution, which is similar to finding an auxiliary link flow pattern in the convex combination method. The outer loop aims to find a new iterative solution based on the descent direction and the step-size corresponding to the auxiliary solution obtained from the inner loop. For more details of deriving the descent direction and step-size determination, please refer to Appendix B.

#### 4. NUMERICAL EXAMPLES

In this section, we use a small network to demonstrate the essential ideas of the proposed model, and a medium network to show the applicability of the proposed solution algorithm.

##### 4.1. Example 1: a small network

The simple network, depicted in Figure 1, consists of six nodes, seven links, and four O-D pairs. We adopt the commonly used BPR function in Equation (19) with parameters  $\beta=0.15$  and  $n=4$ . Link free-flow travel time and capacity are also provided in Figure 1.

We assume the random O-D demands follow the lognormal distribution, where the expected value follows the elastic demand function in Equation (24), and the variance-to-mean ratios (VMR) of all O-D demands are equal to 0.3.

$$q_i^w = r_i(q_{\max}^w - u_i^w), \forall w \in W, i \in I, \tag{24}$$

where  $q_i^w$  is the expected demand of user class  $i$  between O-D pair  $w$ ,  $q_{\max}^w$  is the maximum (or potential) demand between O-D pair  $w$ ,  $u_i^w$  is the minimal METT of all routes between O-D pair  $w$  of user class  $i$ , and  $r_i$  is the proportion of user class  $i$  in the travel demand between O-D pair  $w$ , i.e.,  $\sum_i r_i = 1$ . The maximal demand of each O-D pair and the composition of each route are shown in Table III. Travelers are partitioned into four user classes with the confidence level ranging from 50% to 95% associated with the O-D demand proportions as shown in Table IV.

*Equilibrium results.* The equilibrium results of the proposed model are presented in Table V. As expected, the equilibrium results satisfy the following basic requirements:

- *The METE conditions:* the METTs on all used routes for each O-D pair and each user class are equal and not greater than those of unused routes. For example, the METTs of route 2 for user classes 1–3 in O-D pair (1, 3) are greater than those of route 1, and consequently, travelers of user classes 1–3 only use route 1, whereas travelers in user class 4 use both routes because of their equal METTs (i.e., 12.37) at that confidence level.
- *The elastic demand functions:* the actual travel demand for each O-D pair and each user class satisfies the elastic demand function with respect to the corresponding equilibrium O-D METT. For example, the equilibrium METT for O-D pair (1, 3) and user class 4 is 12.37, which gives the equilibrium travel demand  $q_4^{(1,3)} = r_4 (q_{\max}^{(1,3)} - u_4^{(1,3)}) = 0.4 \times (60 - 12.37) = 19.05$ .
- *The conservation constraints:* the route flows for each O-D pair and each user class are feasible. Using the same example earlier, the summation of route flows (i.e., 4.55 + 14.50) for O-D pair (1, 3) and user class 4 equals the actual travel demand (i.e., 19.05) determined using the aforementioned elastic demand function.

Besides, according to the equivalence property in Appendix A,  $(\mathbf{f}^*, \mathbf{q}^*)$  is the solution to the VI problem if and only if it is a solution to the linear programming model (Equation (A.1)). For the equilibrium results shown in Table V, we have  $\boldsymbol{\eta}(\mathbf{f}^*)^T \mathbf{f}^* - \mathbf{D}^{-1}(\mathbf{q}^*)^T \mathbf{q}^* = 9.69\text{e-}7 \approx 0$ . Thus, as expected, the optimal route-based total system METT  $\boldsymbol{\eta}(\mathbf{f}^*)^T \mathbf{f}^*$  is quite close to the optimal O-D-based total system METT  $\mathbf{u}^{*T} \mathbf{q}^* = \mathbf{D}^{-1}(\mathbf{q}^*)^T \mathbf{q}^*$ . In addition, the optimal values of the Lagrangian multiplier vector  $\boldsymbol{\pi}^*$  associated with the conservation constraints are equal to the minimal O-D METT vector  $\mathbf{u}^*$ , which is also consistent with the well-known duality theory.

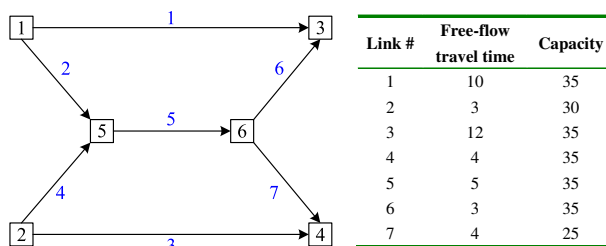


Figure 1. Example network 1.

Table III. Composition of routes and demand distribution.

O-D pair	Demand distribution	Route	Sequence of links
O-D (1, 3)	$q_{\max} = 60, \text{VMR} = 0.3$	1	1
		2	2-5-6
O-D (1, 4)	$q_{\max} = 15, \text{VMR} = 0.3$	3	2-5-7
O-D (2, 3)	$q_{\max} = 25, \text{VMR} = 0.3$	4	4-5-6
O-D (2, 4)	$q_{\max} = 50, \text{VMR} = 0.3$	5	4-5-7
		6	3

O-D, origin–destination; VMR, variance-to-mean ratio.

Table IV. Classification of users in Example 1.

User class	Confidence level (%)	Proportion of demand (%)
1	50	10
2	65	20
3	80	30
4	95	40
Sum		100

Table V. Equilibrium flow and demand pattern of the proposed model.

O-D pair	No. of route	User class	Flow	METT	Demand
(1, 3)	1	1	4.83	11.72	1
		2	9.63	11.86	
		3	14.39	12.03	2
		4	4.55	12.37	
	2	1	0.00	12.04	3
		2	0.00	12.11	
		3	0.00	12.20	4
		4	14.50	12.37	
(1, 4)	3	1	0.21	12.89	0.21
		2	0.41	12.95	0.41
		3	0.59	13.04	0.59
		4	0.72	13.21	0.72
(2, 3)	4	1	1.20	13.03	1.20
		2	2.38	13.10	2.38
		3	3.54	13.19	3.54
		4	4.66	13.36	4.66
(2, 4)	5	1	0.00	13.88	1
		2	0.00	13.94	
		3	0.00	14.03	2
		4	4.94	14.19	
	6	1	3.64	13.58	3
		2	7.26	13.71	
		3	10.84	13.87	4
		4	9.39	14.19	

O-D, origin–destination; METT, mean-excess travel time.

From Table V, we can also see that route METT is increasing with the confidence level. The increase of METT on route 1 is sharper than that on route 2 because of its larger variance of travel time. Route 1 has a smaller mean travel time but a larger variance, whereas route 2 has a larger mean travel time but a smaller variance. When the confidence level is less than 95%, route 1 has a lower METT than that on route 2, and thus, all travelers of classes 1–3 only use route 1. With the increase of the confidence level, the METTs on routes 1 and 2 gradually get close to each other. When the confidence level reaches 95%, travelers of user class 4 use both routes because of the same METT (12.37). The aforementioned equilibrium results indicate that considering both reliability and unreliability requirements of travel time variability may have a more significant effect on route choice decisions for the more risk-averse travelers.

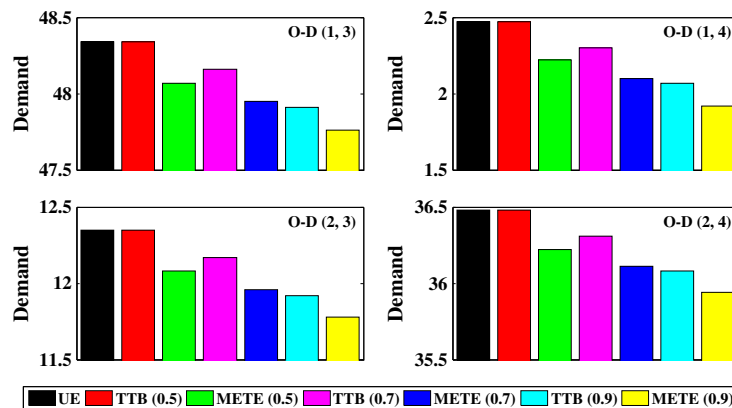


Figure 2. Elastic demands from different traffic equilibrium models: UE, user equilibrium; TTB, travel time budget; METE, mean-excess traffic equilibrium. Note: TTB (0.5): the TTB model with the confidence level of 50%.

*Elastic demand under different route choice criteria.* In the following, we examine the effect of different route choice criteria on the actual travel demand. The expected travel demands obtained from the UE, TTB, and METE models with a *single user class* (i.e., the same confidence level) are compared in Figure 2. From these results, we have the following observations:

- As expected, the optimal travel demand pattern from the TTB model with the confidence level of 0.5 is equal to that from the UE model, which further validates the correctness of the results.
- The travel demands from the UE model are larger than those from both risk-averse models (i.e., TTB and METE models). This means that ignoring travel time variability will overestimate the travel demand level.
- For a particular confidence level, the optimal travel demands from the TTB model are always larger than those from the METE model. This result indicates that ignoring the unreliability aspect of travel time variability in the TTB model may lead to a biased overestimation of the actual travel demand level.
- With the increase of users' confidence level, the actual demand from the TTB (or METE) model is always decreasing. This result implies that more conservative travelers are more likely to cancel trips to hedge against travel time variability.

*Effect of travelers' classification.* Recall that travelers are classified according to their confidence levels, and each class corresponds to a certain demand proportion (see Equation (24)). Thus, travelers' classification is related to the confidence level combination and user proportion combination. In this section, two experiments are conducted to obtain insights into the effect of travelers' classification: (1) components of METT under *different confidence levels* and (2) demand patterns under *different user proportion combinations*.

In Experiment (1), we compare the mean travel time (MTT), buffer travel time (BTT), and EED under different confidence levels. We continue to use the same combination of confidence levels in Table IV but set *equal demand proportion for all classes* (i.e., 25%). For demonstration purpose, the components of METTs on routes 1 and 6 under the aforementioned setting are shown in Figure 3.

We can see that (a) the MTT is independent of the confidence level, and the BTT under the confidence level of 50% equals 0 for user class 1; (b) with the increase of travelers' confidence level (i.e., from class 1 to class 4), both the BTT and the summation of BTT and EED are always increasing. This means that more risk-averse travelers will add a larger travel time to ensure more on-time arrivals and also to avoid worse trip times; and (c) the EED (i.e., the difference between METT and TTB) is decreasing with the increase of confidence level. This decrease is attributed to the fact that under lower confidence levels, if travelers cannot arrive at their destinations within the TTB, the EED could be

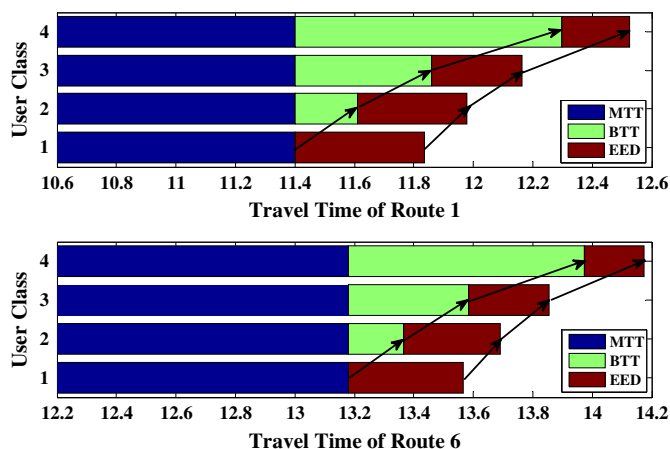


Figure 3. Components of mean-excess travel time under different confidence levels. MTT, mean travel time; BTT, buffer travel time; EED, expected excess delay.

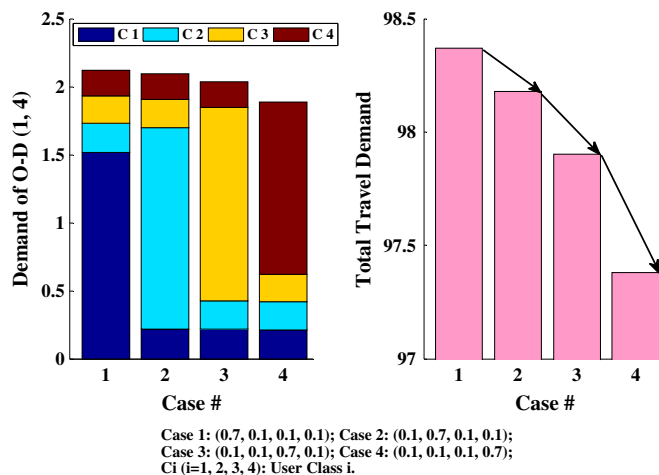


Figure 4. Origin-destination (O-D) demand and total demand under different proportion combinations.

large. However, with the increase of confidence level, the distribution tail beyond the TTB value is gradually decreasing.

Recall that in Figure 2, we examined the travel demand obtained from different traffic equilibrium models with a *single user class*. Here we conduct Experiment (2) to investigate the aggregate effect of *different user proportion combinations* on the actual travel demand. Four cases with the *same combination of confidence levels* (50%, 65%, 80%, 95%) as in Table IV but with *different combinations of user class proportions* are compared. Again for demonstration purpose, we only show the demand of O-D pair (1, 4) and the total travel demand (i.e., the summation of all O-D pair demands for all user classes) in Figure 4. In Case 1, risk-neutral travelers with a confidence level of 50% dominate the four-class user group; in Case 4, more risk-averse travelers with a confidence level of 95% dominate the user group.

From Figure 4, we can observe that from Case 1 to Case 4, the actual demand of O-D pair (1, 4) is strictly decreasing as shown in the left panel. Similar results also occur for the other O-D pairs. Thus, the total travel demand is also decreasing as shown in the right panel. In addition, the reduction from Case 3 to Case 4 is the largest for both the O-D demand and total demand. The reason is that Case 4 is dominated by the most risk-averse class 4 with a confidence level of 95%. This means the MC user-group dominated by the more conservative travelers is more influenced by travel time variability and will accordingly cancel more trips. This result is also consistent with the result under a single user class presented in Figure 2.

#### 4.2. Example 2: Sioux Falls network

In this section, we use the well-known Sioux Falls network to demonstrate the applicability of the proposed algorithm to medium networks. This network contains 24 nodes, 76 links, and 550 O-D pairs. The network topology and link performance parameters are available in the study conducted by Leblanc [19]. We use the standard BPR function in Equation (19) with parameters  $\beta=0.15$  and  $n=4$ . For simplicity, we use a behaviorally generated working route set from Bekhor *et al.* [20]. In this route set, the total number of routes is 3441, the maximum number of routes for any O-D pair is 13, and the average number of routes is 6.3 per O-D pair. The random O-D demands are assumed to follow the lognormal distribution, where the expected value follows the elastic demand function in Equation (24),

Table VI. Classification of travelers in Example 2.

User class	Confidence level (%)	Proportion (%)
1	70	30
2	90	70

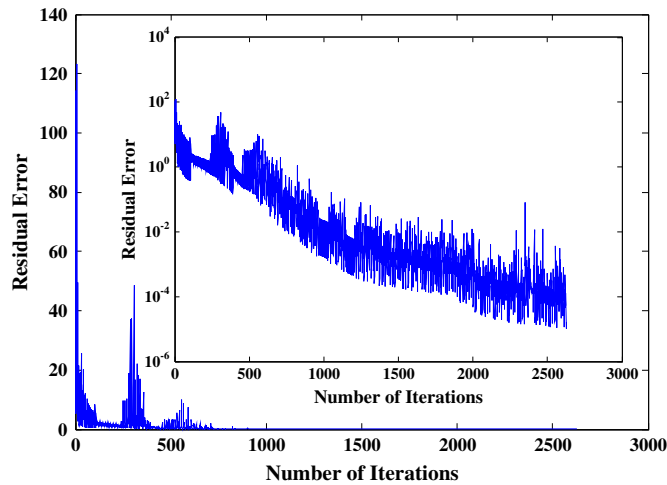


Figure 5. Convergence curve of the modified alternating direction method.

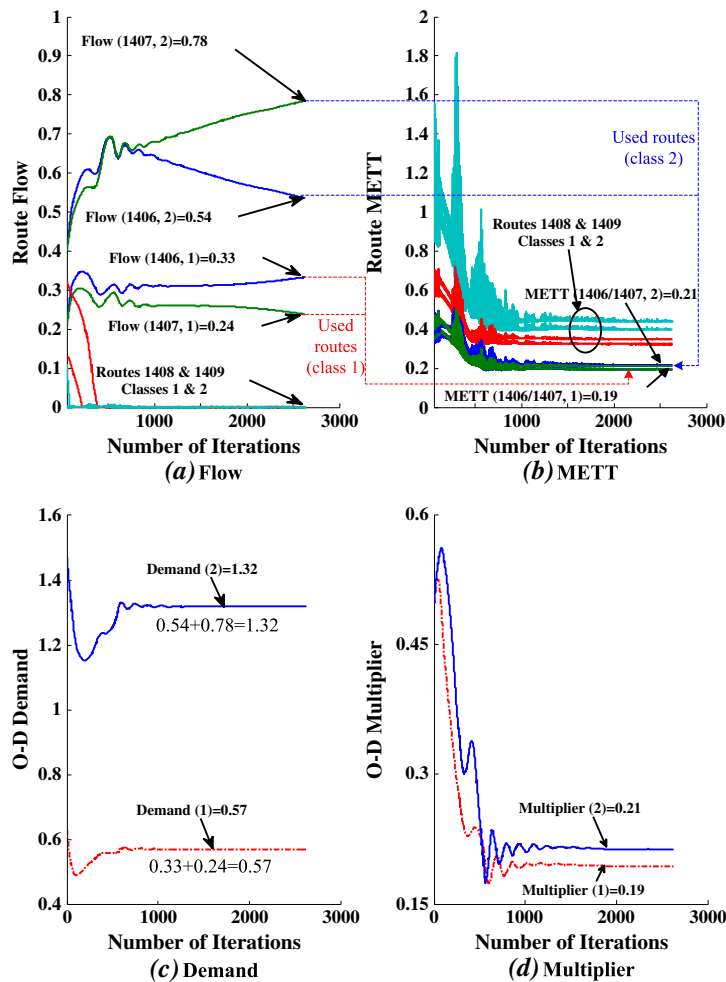


Figure 6. Evolution process of route flows, mean-excess travel times (METTs), demands, and multipliers. Note: Flow (1406, 1): flow on route 1406 of class 1; Demand (1): actual demand of class 1.

and the VMRs of all O-D demands are equal to 0.3. The maximal O-D demand is the same as the O-D trip table in the study by Bekhor *et al.* [20]. We consider two user classes as shown in Table VI.

Table VII. Comparison of network-level performance measures.

Model	User equilibrium	Travel time budget	Mean-excess traffic equilibrium
Total network travel time	37.73 (14.33%)	34.21 (3.67%)	33.00
Total network travel demand	301.12 (4.05%)	293.00 (1.24%)	289.41

The parameters used in the MAD method are set as follows:  $\varepsilon = 1e-5$ ,  $\beta_0 = 0.1$ ,  $\mu = 0.6$ ,  $\gamma = 1.95$ , and  $\delta = 0.75$ . We use the residual error function  $\|\mathbf{r}(\mathbf{x}^k, \beta_k)\|/\beta_k$  as the convergence measure. The initial demand for a given O-D pair and a given user class is set to be the maximal demand of this O-D pair multiplied by the proportion of this user class. The initial route flows for a given O-D pair and a given user class are set to be the initial O-D demand of this user class divided by the number of routes connecting this O-D pair. The algorithm is coded in MATLAB<sup>®</sup> 7.5 and run on a personal TOSHIBA laptop computer with 2.00 G Pentium (R) Dual-Core processor and 1.86 G RAM.

Initially, we show the convergence curve of the MAD method in Figure 5. The algorithm terminates after 2626 iterations, and the CPU time is 73 s. One can see that the residual error fluctuates sharply in the early iterations and stabilizes after 700 iterations. The superior performance mainly owes to the self-adaptive step-size strategy in Steps 2 and 7. The step-size  $\beta_k$  can adjust itself automatically according to the route flows, METTs, and demands generated in the previous iterations.

To further demonstrate the convergence characteristics of the MAD method, we examine the evolution process of route flows, route METTs, O-D demands, and O-D multipliers of different user classes. For demonstration purpose, we only show the results on the four routes between O-D pair (10, 14) in Figure 6. One can see that the required accuracy (i.e.,  $1e-5$ ) can be achieved within acceptable computational efforts. Also, as expected, the route flows, METTs, travel demands, and multipliers satisfy the METT-based UE conditions, conservation constraints, and elastic demand functions.

Finally, we compare the network-level performance corresponding to the UE, TTB, and METE models. All three models use the same elastic demand function, travel demand distribution, and user classification. The total network travel time (TNTT) and total network travel demand (TNTD) are shown in Table VII. The percentages shown in parentheses denote the relative differences with respect to the METE model. We can observe that both UE and TTB models overestimate the TNTT and TNTD, which may lead to a biased network performance assessment. Thus, both reliability and unreliability aspects of travel time variability should be simultaneously considered in travelers' travel choice and route choice decisions under uncertainty.

## 5. CONCLUSIONS AND FUTURE RESEARCH

In this study, we developed a MC-METE model with elastic demand. METT is adopted as a route choice criterion to consider both reliability (on-time arrival) and unreliability (late arrival) aspects of travel time variability. This model explicitly considers heterogeneous risk-aversion attitudes and elastic demand in the METE framework. Specifically, each user class has their own risk attitude toward travel time variability. The actual demand of each user class and each O-D pair is dependent on the minimal O-D METT. The proposed model was formulated as a VI problem and solved using a route-based MAD method to handle the elastic demand and heterogeneous risk-aversion considerations. Numerical examples were also provided to illustrate the essential ideas of the proposed model and the applicability of the MAD method to medium networks.

The analysis results indicated that (1) on the *route choice* level, considering both reliability and unreliability requirements of travel time variability has a more significant effect on route choice decisions for the more risk-averse travelers; (2) on the *travel choice* level, more conservative travelers (or the MC user-group dominated by the more conservative travelers) are more likely to cancel trips to hedge against travel time variability; and (3) on the *network performance* level, ignoring reliability and unreliability aspects of travel time variability can overestimate the TNTT and TNTD, which may lead to a biased network performance assessment.

For future research, uncertainties from both demand fluctuation and capacity degradation should be simultaneously considered. We plan to explore the characterization methods of travel demand uncertainty and the effect of different travel demand distributions (e.g., Gamma, Weibull, Burr) on the equilibrium flow patterns as well as network-wide performance measures. For solution algorithm, embedding a column generation scheme (e.g., [21]) within the route-based MAD method for testing large networks is needed for practical applications of the proposed traffic equilibrium model. In addition, we plan to explore the mathematical properties of METT (e.g., monotonicity), which are useful for developing more efficient solution algorithms. It will also be useful to enhance the modeling capability by extending the current model to consider the effects of travel time variability and heterogeneous risk-aversion attitudes on other travel choice dimensions (e.g., destination choice and mode choice). The combined (or integrated) travel demand models are directly related to the selection of different risk-taking choice criteria. We will examine the effect of using different risk-taking criteria (e.g., TTB and METT) on other travel choice decisions in the future.

## 6. LIST OF SYMBOLS AND ABBREVIATIONS

### 6.1. Abbreviations

BPR	Bureau of public roads
BTT	Buffer travel time
EED	Expected excess delay
MAD	Modified alternating direction
MC-METE-ED	Multi-class mean-excess traffic equilibrium with elastic demand
METE	Mean-excess traffic equilibrium
METT	Mean-excess travel time
MTT	Mean travel time
TNTD	Total network travel demand
TNTT	Total network travel time
TTB	Travel time budget
UE	User equilibrium
VI	Variational inequality
VMR	Variance-to-mean ratio

### 6.2. Symbols

$N$	Set of nodes
$A$	Set of links
$W$	Set of O-D pairs
$I$	Set of all user classes
$P^w$	Set of routes connecting O-D pair $w$
$P$	Set of $P^w$
$T_p^w$	Travel time on route $p$ between O-D pair $w$
$f_{p,i}^w$	Route flow of user class $i$ on route $p$ between O-D pair $w$
$\alpha_i$	Confidence level of user class $i$
$\zeta_{p,i}^w$	Travel time budget of user class $i$ on route $p$ between O-D pair $w$
$\eta_{p,i}^w$	Mean-excess travel time of user class $i$ on route $p$ between O-D pair $w$
$q_i^w$	Travel demand of user class $i$ between O-D pair $w$
$D_i^w(\cdot)$	Travel demand function of user class $i$ between O-D pair $w$
$u_i^w$	Minimal METT of user class $i$ between O-D pair $w$
$\xi$	Vector of route TTBs $\xi = (\dots, \zeta_{p,i}^w, \dots)^T$
$\eta$	Vector of route METTs $\eta = (\dots, \eta_{p,i}^w, \dots)^T$
$\mathbf{f}$	Vector of route flows $\mathbf{f} = (\dots, f_{p,i}^w, \dots)^T$

$\mathbf{q}$	Vector of travel demands, $\mathbf{q} = (\dots, q_i^w, \dots)^T$
$\mathbf{u}$	Vector of minimal METTs, $\mathbf{u} = (\dots, u_i^w, \dots)^T$
$\Lambda$	O-D pair-route incidence matrix

## ACKNOWLEDGEMENT

The authors are grateful to Prof William Lam (Editor of Journal of Advanced Transportation) and two referees for providing useful comments and suggestions for improving the quality and clarity of the paper. The work of the first author was supported by the China Scholarship Council. The work of the second author was supported by a CAREER grant from the National Science Foundation of the United States (CMS-0134161) and an Oriental Scholar Professorship Program sponsored by the Shanghai Ministry of Education in China to Tongji University.

## REFERENCES

1. van Lint JWC, van Zuylen HJ, Tu H. Travel time unreliability on freeways: why measures based on variance tell only half the story. *Transportation Research Part A* 2008; **42**(1):258–277.
2. Asensio J, Matas A. Commuters' valuation of travel time variability. *Transportation Research Part E* 2008; **44**(6):1074–1085.
3. Liu H, Recker W, Chen A. Uncovering the contribution of travel time reliability to dynamic route choice using real-time loop data. *Transportation Research Part A* 2004; **38**(6):435–453.
4. Bell MGH, Cassir C. Risk-averse user equilibrium traffic assignment: an application of game theory. *Transportation Research Part B* 2002; **36**(8):671–681.
5. Mirchandani P, Soroush H. Generalized traffic equilibrium with probabilistic travel times and perceptions. *Transportation Science* 1987; **21**:133–152.
6. Zhang C, Chen X, Sumalee A. Robust Wardrop's user equilibrium assignment under stochastic demand and supply: expected residual minimization approach. *Transportation Research Part B* 2011; **45**(3):534–552.
7. Xu H, Lou Y, Yin Y, Zhou J. A prospect-based user equilibrium model with endogenous reference points and its application in congestion pricing. *Transportation Research Part B* 2011; **45**(2):311–328.
8. Lo HK, Luo XW, Siu BWY. Degradable transport network: travel time budget of travelers with heterogeneous risk aversion. *Transportation Research Part B* 2006; **40**(9):792–806.
9. Shao H, Lam WHK, Meng Q, Tam ML. Demand-driven traffic assignment problem based on travel time reliability. *Transportation Research Record* 2006a; **1985**:220–230.
10. Shao H, Lam WHK, Tam ML. A reliability-based stochastic traffic assignment model for network with multiple user classes under uncertainty in demand. *Networks and Spatial Economics* 2006b; **6**(3–4):173–204.
11. Sumalee A, Uchida K, Lam WHK. Stochastic multi-modal transport network under demand uncertainties and adverse weather condition. *Transportation Research Part C* 2011; **19**:338–350.
12. Szeto WY, Solayappan M, Jiang Y. Reliability-based transit assignment for congested stochastic transit networks. *Computer-Aided Civil and Infrastructure Engineering* 2011b; **26**(4):311–326.
13. Zhang Y, Lam WHK, Sumalee A, Lo HK, Tong CO. The multi-class schedule-based transit assignment model under network uncertainties. *Public Transport* 2010; **2**(1–2):69–86.
14. Szeto WY, Jiang Y, Sumalee A. A cell-based model for multi-class doubly stochastic dynamic traffic assignment. *Computer-Aided Civil and Infrastructure Engineering* 2011a; **26**(8):595–611.
15. Watling D. User equilibrium traffic network assignment with stochastic travel times and late arrival penalty. *European Journal of Operational Research* 2006; **175**(3):1539–1556.
16. Chen A, Zhou Z. The  $\alpha$ -reliable mean-excess traffic equilibrium model with stochastic travel times. *Transportation Research Part B* 2010; **44**(4):493–513.
17. Zhou Z, Chen A. Comparative analysis of three user equilibrium models under stochastic demand. *Journal of Advanced Transportation* 2008; **42**(3):239–263.
18. Han DR. A modified alternating direction method for variational inequality problems. *Applied Mathematics and Optimization* 2002; **45**(1):63–74.
19. Leblanc LJ. Mathematical programming algorithms for large-scale network equilibrium and network design problems. PhD Thesis, Northwestern University, 1973.
20. Bekhor S, Toledo T, Prashker JN. Effects of choice set size and route choice models on path-based traffic assignment. *Transportmetrica* 2008; **4**(2):117–133.
21. Chen BY, Lam WHK, Sumalee A, Shao H. An efficient solution algorithm for solving multi-class reliability-based traffic assignment problem. *Mathematical and Computer Modelling* 2011a; **54**(5–6):1428–1439.
22. Facchinei F, Pang JS. *Finite-Dimensional Variational Inequalities and Complementarity Problems*. Springer: New York, 2003.
23. Gass SI. *Linear Programming: Methods and Applications*. McGraw-Hill: New York, 1985.

24. Siu BWY, Lo HK. Doubly uncertain transport network: degradable link capacity and perception variations in traffic conditions. *Transportation Research Record* 2006; **1964**:56–69.
25. Lam WHK, Shao H, Sumalee A. Modeling impacts of adverse weather conditions on a road network with uncertainties in demand and supply. *Transportation Research Part B* 2008; **42**(10):890–910.
26. Shao H, Lam WHK, Tam ML, Yuan XM. Modeling rain effects on risk-taking behaviors of multi-user classes in road network with uncertainty. *Journal of Advanced Transportation* 2008; **42**(3):265–290.
27. Siu BWY, Lo HK. Doubly uncertain transportation network: degradable capacity and stochastic demand. *European Journal of Operational Research* 2008; **191**(1):166–181.
28. Chen A, Zhou Z, Lam WHK. Modeling stochastic perception error in the mean-excess traffic equilibrium model with stochastic travel times. *Transportation Research Part B* 2011b; **45**(10):1619–1640.

## APPENDIX A

Appendix A presents the qualitative properties of the proposed VI problem, including the existence of a solution to the VI problem, and its equivalence to the MC-METE conditions with elastic demand.

**Proposition 1. Existence** *The proposed VI problem admits at least one solution under the assumptions that the METT on each route between each O-D pair for each user class is positive and continuous with respect to its route flow, and the inverse demand function between each O-D pair for each user class is non-negative and continuous with respect to its travel demand.*

*Proof.* The feasible set  $\Omega_{\mathbf{f}\mathbf{q}}$  is non-empty, closed, and convex. Moreover, the METT  $\boldsymbol{\eta}(\mathbf{f})$  is positive and continuous with respect to  $\mathbf{f}$ , and the inverse travel demand function  $\mathbf{D}^{-1}(\mathbf{q})$  is non-negative and continuous with respect to  $\mathbf{q}$ . According to Corollary 2.2.5 in the study conducted by Facchinei and Pang [22], the aforementioned VI problem thus has at least one solution. This completes the proof.  $\blacksquare$

**Proposition 2. Equivalence;** *The solution to the proposed VI problem is equivalent to the MC-METE-ED conditions.*

*Proof.* Equation (17) is equivalent to  $\boldsymbol{\eta}(\mathbf{f}^*)^T \mathbf{f} - \mathbf{D}^{-1}(\mathbf{q}^*)^T \mathbf{q} \geq \boldsymbol{\eta}(\mathbf{f}^*)^T \mathbf{f}^* - \mathbf{D}^{-1}(\mathbf{q}^*)^T \mathbf{q}^*$ ,  $\forall (\mathbf{f}, \mathbf{q}) \in \Omega_{\mathbf{f}\mathbf{q}}$ . Thus,  $(\mathbf{f}^*, \mathbf{q}^*)$  is a solution to the VI problem (17)–(18) if and only if it is a solution to the following linear programming model with the same solution vectors (i.e., route flow and travel demand):  $\blacksquare$

$$\min_{(\mathbf{f}, \mathbf{q}) \in \Omega_{\mathbf{f}\mathbf{q}}} \boldsymbol{\eta}(\mathbf{f}^*)^T \mathbf{f} - \mathbf{D}^{-1}(\mathbf{q}^*)^T \mathbf{q}. \quad (\text{A.1})$$

Using the relationship between the primal and dual solutions of linear programming (Equation (A.1)) [23], we can obtain

$$f_{p,i}^{w,*} \left( \eta_{p,i}^w(\mathbf{f}^*) - u_i^w \right) = 0, \forall p \in P^w, w \in W, i \in I, \quad (\text{A.2})$$

$$\eta_{p,i}^w(\mathbf{f}^*) - u_i^w \geq 0, \forall p \in P^w, w \in W, i \in I, \quad (\text{A.3})$$

$$f_{p,i}^{w,*} \geq 0, \forall p \in P^w, w \in W, i \in I, \quad (\text{A.4})$$

$$q_i^{w,*} \left( u_i^w - D_i^{w,-1}(q_i^{w,*}) \right) = 0, \forall w \in W, i \in I, \quad (\text{A.5})$$

$$u_i^w - D_i^{w,-1}(q_i^{w,*}) \geq 0, \forall w \in W, i \in I, \quad (\text{A.6})$$

$$q_i^{w,*} \geq 0, \forall w \in W, i \in I. \quad (\text{A.7})$$

Equations (A.2)–(A.4) ensure that the equilibrium route flow pattern satisfies the METT-based UE conditions. From Equations (A.5)–(A.7), the travel demand functions also give the equilibrium demand pattern. Thus, the MC-METE-ED conditions are satisfied. This completes the proof.

APPENDIX B.

Some formulae used in the solution procedure are derived as follows.

Define  $\mathbf{r}(\mathbf{x}, \beta)$  as

$$\begin{aligned} \mathbf{r}(\mathbf{x}, \beta) = \begin{pmatrix} \mathbf{r}_1(\mathbf{x}, \beta) \\ \mathbf{r}_2(\mathbf{x}, \beta) \\ \mathbf{r}_3(\mathbf{x}, \beta) \end{pmatrix} &= \begin{pmatrix} \mathbf{f} - P_{R_+^{|\rho|}}[\mathbf{f} - \beta(\boldsymbol{\eta}(\mathbf{f}) - \boldsymbol{\Lambda}^T(\boldsymbol{\pi} - \beta(\boldsymbol{\Lambda}\mathbf{f} - \mathbf{q})))] \\ \mathbf{q} - P_{R_+^{|\omega|}}[\mathbf{q} - \beta(-\mathbf{D}^{-1}(\mathbf{q}) + (\boldsymbol{\pi} - \beta(\boldsymbol{\Lambda}\mathbf{f} - \mathbf{q})))] \\ \beta(\boldsymbol{\Lambda}\mathbf{f} - \mathbf{q}) \end{pmatrix} \\ &= \begin{pmatrix} \mathbf{f} - P_{R_+^{|\rho|}}[\mathbf{f} - \beta\mathbf{g}_1(\mathbf{x})] \\ \mathbf{q} - P_{R_+^{|\omega|}}[\mathbf{q} - \beta\mathbf{g}_2(\mathbf{x})] \\ \mathbf{g}_3(\mathbf{x}) \end{pmatrix}. \end{aligned} \tag{B.1}$$

Let  $(\mathbf{f}^*, \mathbf{q}^*, \boldsymbol{\pi}^*)$  be an arbitrary solution of the VI problem.

(1) According to the basic property of the projection operator, we have

$$\left\{ \mathbf{f} - \beta\mathbf{g}_1(\mathbf{x}) - P_{R_+^{|\rho|}}[\mathbf{f} - \beta\mathbf{g}_1(\mathbf{x})] \right\}^T \left\{ P_{R_+^{|\rho|}}[\mathbf{f} - \beta\mathbf{g}_1(\mathbf{x})] - \mathbf{f}^* \right\} \geq 0, \tag{B.2}$$

$$\left\{ \mathbf{q} - \beta\mathbf{g}_2(\mathbf{x}) - P_{R_+^{|\omega|}}[\mathbf{q} - \beta\mathbf{g}_2(\mathbf{x})] \right\}^T \left\{ P_{R_+^{|\omega|}}[\mathbf{q} - \beta\mathbf{g}_2(\mathbf{x})] - \mathbf{q}^* \right\} \geq 0. \tag{B.3}$$

(2) Based on the monotonicity assumption, we have

$$\beta \left\{ \boldsymbol{\eta} \left( P_{R_+^{|\rho|}}[\mathbf{f} - \beta\mathbf{g}_1(\mathbf{x})] \right) - \boldsymbol{\eta}(\mathbf{f}^*) \right\}^T \left\{ P_{R_+^{|\rho|}}[\mathbf{f} - \beta\mathbf{g}_1(\mathbf{x})] - \mathbf{f}^* \right\} \geq 0, \tag{B.4}$$

$$\beta \left\{ -\mathbf{D}^{-1} \left( P_{R_+^{|\omega|}}[\mathbf{q} - \beta\mathbf{g}_2(\mathbf{x})] \right) + \mathbf{D}^{-1}(\mathbf{q}^*) \right\}^T \left\{ P_{R_+^{|\omega|}}[\mathbf{q} - \beta\mathbf{g}_2(\mathbf{x})] - \mathbf{q}^* \right\} \geq 0. \tag{B.5}$$

(3) Because  $(\mathbf{f}^*, \mathbf{q}^*, \boldsymbol{\pi}^*)$  is a solution to the VI problem, we obtain

$$\beta \left\{ \boldsymbol{\eta}(\mathbf{f}^*) - \boldsymbol{\Lambda}^T \boldsymbol{\pi}^* \right\}^T \left\{ P_{R_+^{|\rho|}}[\mathbf{f} - \beta\mathbf{g}_1(\mathbf{x})] - \mathbf{f}^* \right\} \geq 0, \tag{B.6}$$

$$\beta \left\{ -\mathbf{D}^{-1}(\mathbf{q}^*) + \boldsymbol{\pi}^* \right\}^T \left\{ P_{R_+^{|\omega|}}[\mathbf{q} - \beta\mathbf{g}_2(\mathbf{x})] - \mathbf{q}^* \right\} \geq 0. \tag{B.7}$$

Note that  $\mathbf{f} - \mathbf{r}_1(\mathbf{x}, \beta) = P_{R_+^{|\rho|}}[\mathbf{f} - \beta\mathbf{g}_1(\mathbf{x})]$  and  $\mathbf{q} - \mathbf{r}_2(\mathbf{x}, \beta) = P_{R_+^{|\omega|}}[\mathbf{q} - \beta\mathbf{g}_2(\mathbf{x})]$ , then adding Equations (B.2), (B.4), and (B.6), we have

$$\begin{aligned} &\left\{ \mathbf{r}_1(\mathbf{x}, \beta) - \beta[\boldsymbol{\eta}(\mathbf{f}) - \boldsymbol{\eta}(\mathbf{f} - \mathbf{r}_1(\mathbf{x}, \beta))] - \beta\boldsymbol{\Lambda}^T \mathbf{r}_3(\mathbf{x}, \beta) + \beta\boldsymbol{\Lambda}^T(\boldsymbol{\pi} - \boldsymbol{\pi}^*) \right\}^T \\ &(\mathbf{f} - \mathbf{f}^* - \mathbf{r}_1(\mathbf{x}, \beta)) \geq 0. \end{aligned} \tag{B.8}$$

Similarly by adding Equations (B.3), (B.5), and (B.7), we can get

$$\begin{aligned} & \{\mathbf{r}_2(\mathbf{x}, \beta) - \beta[-\mathbf{D}^{-1}(\mathbf{q}) + \mathbf{D}^{-1}(\mathbf{q} - \mathbf{r}_2(\mathbf{x}, \beta))] + \beta\mathbf{r}_3(\mathbf{x}, \beta) - \beta(\boldsymbol{\pi} - \boldsymbol{\pi}^*)\}^T \\ & (\mathbf{q} - \mathbf{q}^* - \mathbf{r}_2(\mathbf{x}, \beta)) \geq 0. \end{aligned} \quad (\text{B.9})$$

Adding Equations (B.8) and (B.9), we then have

$$\begin{aligned} & \begin{pmatrix} \mathbf{f} - \mathbf{f}^* \\ \mathbf{q} - \mathbf{q}^* \\ \boldsymbol{\pi} - \boldsymbol{\pi}^* \end{pmatrix}^T \begin{pmatrix} \mathbf{r}_1(\mathbf{x}, \beta) - \beta[\boldsymbol{\eta}(\mathbf{f}) - \boldsymbol{\eta}(\mathbf{f} - \mathbf{r}_1(\mathbf{x}, \beta))] - \beta\boldsymbol{\Lambda}^T \mathbf{r}_3(\mathbf{x}, \beta) \\ \mathbf{r}_2(\mathbf{x}, \beta) - \beta[-\mathbf{D}^{-1}(\mathbf{q}) + \mathbf{D}^{-1}(\mathbf{q} - \mathbf{r}_2(\mathbf{x}, \beta))] + \beta\mathbf{r}_3(\mathbf{x}, \beta) \\ \mathbf{r}_3(\mathbf{x}, \beta) - \beta\boldsymbol{\Lambda} \mathbf{r}_1(\mathbf{x}, \beta) + \beta\mathbf{r}_2(\mathbf{x}, \beta) \end{pmatrix} \geq \quad (\text{B.10}) \\ & \|\mathbf{r}_1(\mathbf{x}, \beta)\|^2 + \|\mathbf{r}_2(\mathbf{x}, \beta)\|^2 - \beta(\mathbf{r}_1(\mathbf{x}, \beta))^T [\boldsymbol{\eta}(\mathbf{f}) - \boldsymbol{\eta}(\mathbf{f} - \mathbf{r}_1(\mathbf{x}, \beta))] - \\ & \beta(\mathbf{r}_2(\mathbf{x}, \beta))^T [-\mathbf{D}^{-1}(\mathbf{q}) + \mathbf{D}^{-1}(\mathbf{q} - \mathbf{r}_2(\mathbf{x}, \beta))] - \beta(\mathbf{r}_3(\mathbf{x}, \beta))^T \boldsymbol{\Lambda} \mathbf{r}_1(\mathbf{x}, \beta) + \\ & \beta(\mathbf{r}_3(\mathbf{x}, \beta))^T \mathbf{r}_2(\mathbf{x}, \beta) \equiv \varphi(\mathbf{x}, \beta). \end{aligned}$$

The self-adaptive step-size strategy in Steps 2 and 7 mainly comes from the right-hand-side term of inequality (Equation (B.10)), and the second term on the left-hand side of inequality (Equation (B.10)) is the search direction in Step 4.